Journal of Molecular Catalysis A: Chemical 355 (2012) 142–154

Contents lists available at SciVerse ScienceDirect

Journal of Molecular Catalysis A: Chemical

journal homepage: www.elsevier.com/locate/molcata

Aldol condensation of benzaldehyde with heptanal to jasminaldehyde over novel Mg–Al mixed oxide on hexagonal mesoporous silica

Ganapati D. Yadav*, Pavankumar Aduri

Department of Chemical Engineering, Institute of Chemical Technology, Matunga, Mumbai 400019, India

ARTICLE INFO

Article history:
Received 9 September 2011
Received in revised form 4 December 2011
Accepted 7 December 2011
Available online 17 December 2011

Keywords:
Hydrotalcite
Hexagonal mesoporous silica
Magnesium–aluminum mixed oxide
Aldol condensation
Jasminaldehyde

ABSTRACT

A novel calcined hydrotalcite supported on hexagonal mesoporous silica (CHT/HMS) was synthesized and characterized by XRD, TG–DTA, pore size analysis, SEM–EDAX, and TEM. It possesses high thermal stability, high adsorption capacity and large surface area. 20% (w/w) CHT/HMS was highly active and selective in aldol-condensation of benzaldehyde with heptanal. A kinetic model was developed and validated against experimental data. Jasminaldehyde selectivity of 86% was obtained with heptanal to benzaldehyde mole ratio of 1:5 at 150 °C by using 20% (w/w) CHT/HMS. The results are explained on the basis of the bi-functional character of CHT/HMS, where the role of the weak acid sites is the activation of benzaldehyde by protonation of the carbonyl group which favors the attack of the enolate heptanal intermediate generated on basic sites. The catalyst is stable and reusable.

1. Introduction

A variety of solid acids have been extensively studied as prospective catalysts for industrial processes. Among them, zeolites have made the greatest impact due to their several applications in petroleum refineries and petrochemical industries [1,2]. However, in contrast with solid acids, comparatively few efforts have gone into studying solid bases as industrial catalysts [1,3–7]. Base catalyzed reactions include alkylation, isomerization, Michael addition, aldol, Knoevenagel and Claisen–Schmidt condensations, which are used for the production of bulk chemicals, fine chemicals, pharmaceuticals, perfumes and flavors. More than 1.5 million tonnes of bulk chemicals are produced annually via processes catalyzed by alkalies such as NaOH, KOH and $Ca(OH)_2$. After the reaction, the alkalies are neutralized with acids and they contribute to ~30% of the product cost, resulting from product separation, purification and waste-water treatment [8–10]. Substitution of homogeneous bases by cleaner heterogeneous catalysts is desirable in consonance with the principles of Green Chemistry. Solid base catalysts are non-stoichiometric, non-corrosive and reusable. They are tunable and easily separable from the reaction mixture with almost zero emission of effluents. Additionally, shape selectivity can also be realized by embedding them on suitable supports, leading to an intriguing activity and selectivity. The mechanism of solid base catalyzed reactions involves anion intermediates. There is a dearth of information in the literature on industrially important reactions catalyzed by heterogeneous base catalysts. Hydrotalcites possess a great potential as solid bases for industrial use [11–15].

Hydrotalcites are mixed oxides having high surface area, phase purity, tunable basicity and structural stability. They have multiple uses such as antacids, ion exchangers, absorbers, catalysts and supports [16]. Hydrotalcites, with a positively charged layered-brucite type of structure, are uncommon in nature but they can be easily synthesized in laboratory. Positive charges are created in the hydrotalcite structure, through replacement of Mg by Al, which are neutralized by interlayer anions such as carbonate, nitrate, hydroxide and chloride. The interlayer anions can also be replaced by other organic and inorganic anions [17]. Hydrotalcites are normally calcined at 500–800 °C to form magnesium and aluminum oxide solid solutions. Calcined Mg–Al hydrotalcite is reported to be very active in various base catalyzed organic reactions [18]. It can be viewed as a porous material possessing several pairs of strong basic site (O^{2-} ion) and Lewis acid site (co-ordinatively unsaturated Al^{3+} ion).

Although basic zeolites have been used in a variety of reactions, they have restrictions in the synthesis of fine chemicals. Micropores of zeolites prevent bulky molecules from reaching the active sites. New families of mesoporous silicas, such as MCM-41 and SBA-15 possess tunable large pore sizes and provide opportunities for their use as supports. Basic mesoporous materials may be prepared by (a) cation exchange with alkali (e.g. Na^+, K^+, Cs^+) metal ions, (b) impregnation with alkali salts solution and calcination, and (c) functionalization with organic groups. Ordered mesoporous materials such as M41S [19], FSM-16 [20], HMS [21], MSU [22], and SBA [23] have been modified to achieve better

* Corresponding author. Tel.: +91 22 3361 1001/1111/22222; fax: +91 22 3361 1002/1020.
E-mail addresses: gdyadav@yahoo.com, gd.yadav@ictmumbai.edu.in (G.D. Yadav).

1381-1169/$ – see front matter © 2011 Elsevier B.V. All rights reserved.
doi:10.1016/j.molcata.2011.12.008

thermal/hydrothermal stability, to create catalytic centers and to use them in nanotechnology [24–27]. Mesoporous materials possessing high thermal stability (up to 1198 K), large surface area (~1000 m^2/g), uniform pore-sizes and substantial adsorption capacity are excellent catalyst supports [28–30]. There is no report in the literature on hydrotalcites supported on mesoporous materials. This work was therefore undertaken.

Jasminaldehyde (or α-amylcinnamaldehyde) is a well-known perfumery product, which is manufactured by the aldol condensation of benzaldehyde and heptanal by using alkaline catalysts in batch processes [31,32]. The reaction is invariably accompanied by self-condensation of heptanal, leading to a major by-product (E)-2-*n*-pentyl-2-*n*-nonenal. Since the boiling point of this by-product is very close to that of jasminaldehyde, it is necessary to minimize the self-condensation by using a selective catalyst and operating parameters to overcome difficult and expensive separation.

Some base catalysts have been reported for the synthesis of jasminaldehyde, such as anion exchange resins [33], potassium carbonate using solid–liquid phase-transfer catalysis (S–L PTC) [34], and also S–L PTC in dry media under microwave irradiation [35]. Heptanal concentration is kept low in this reaction by firstly converting it into a hemiacetal by reaction with methanol. In order to improve selectivity and to suppress self-condensation, a high benzaldehyde to heptanal mole ratio is needed, thereby necessitating large reactors. 1,5,7-Triazabicyclo[4.4.0]dec-5-ene (TBD) immobilized on MCM-41 is also used as a catalyst, which is more stable and shows a better selectivity [36,37]. Solid acids have also been investigated as catalysts. Climent et al. [38] have compared the performance of acidic catalysts such as zeolites (HY and H-β), mesoporous aluminosilicates (Al-MCM-41) and amorphous aluminophosphate (ALPO). ALPO is a bi-functional (acid–base) catalyst which possesses weaker acid sites than zeolites. ALPO showed a very high activity and selectivity to jasminaldehyde. Their work suggests that both acid and base sites are required for this reaction. Yu et al. [39] have reported calcined hydrotalcite as a base catalyst confirming the requirement of bi-functionality.

In the current work, a novel catalyst calcined-hydrotalcite (CHT) supported on hexagonal mesoporous silica (HMS), CHT/HMS, is reported. The catalyst is fully characterized. The activity and selectivity of CHT/HMS are examined by studying the effects of different operating parameters in aldol condensation of benzaldehyde with heptanal. The mechanism and kinetics of both the aldol and self-condensation reactions are deduced. The catalyst is highly selective and robust.

2. Experimental

2.1. Chemicals

Magnesium nitrate (LR grade), aluminum nitrate (LR grade), sodium hydroxide and sodium carbonate were obtained from Merck, India. Commercial grade (95%) ethanol, heptanal and benzaldehyde, all A.R. grade, were procured from M/s. S. D. Fine Chemicals Ltd., Mumbai, India.

Tetraethyl orthosilicate (TEOS) (Fluka) was used as the neutral silica source whereas dodecylamine and hexadecyl amine (Spectrochem Ltd.) were used as the templates in the preparation of HMS.

2.2. Catalyst preparation

2.2.1. Hexagonal mesoporous silica (HMS)

HMS was prepared by using the following procedure: 26 g of hexadecylamine was dissolved in 202 ml of ethanol. To this surfactant solution, 214 ml of deionized water was added dropwise under vigorous stirring conditions. Any precipitate formed during the addition was solubilized by adding additional ethanol which improved the solubility of template. A total of 89 ml of TEOS was added drop by drop in the above solution under vigorous stirring. The reaction mixture was then stirred for additional 4 h after which it was allowed to age for 24 h. The clear liquid above the white colored precipitate was decanted and the precipitate was dried on a glass plate at room temperature. The template was removed by calcining the resulting material at 550 °C [40].

2.2.2. Hydrotalcite (HT) and calcined hydrotalcite (CHT)

HT was prepared by a standard procedure and heat crystallization. A solution of 1 mol magnesium nitrate ($Mg(NO_3)_2{\cdot}6H_2O$) and 0.5 mol aluminum nitrate ($Al(NO_3)_3{\cdot}6H_2O$) was prepared by dissolving the corresponding salts in distilled water. The solution was then co-precipitated by the addition of 50% aqueous solution of 3.5 mol NaOH and Na_2CO_3 (anhydrous 0.943 mol) in distilled water. The addition took about 4 h and was carried out carefully with vigorous stirring at room temperature or below 35 °C. During the addition, the pH of the solution was maintained between 9 and 10. The slurry was cooled to room temperature, filtered and washed with deionized water until the pH of the wash water was 7. After drying at 373 K for 24 h, the solids were calcined at 723 K for 12 h to get CHT [41].

2.2.3. Synthesis of CHT/HMS

A quantity 10 g of HMS was added to 10 ml of an aqueous solution containing 1 mol magnesium nitrate ($Mg(NO_3)_2{\cdot}6H_2O$) and 0.5 mol aluminum nitrate ($Al(NO_3)_3{\cdot}6H_2O$) and stirred vigorously for 30 min at 333 K to form a suspension. The solution was then co-precipitated by the addition of 50% aqueous NaOH (3.5 mol) and Na_2CO_3 (anhydrous 0.943 mol) in 10 ml distilled water. The addition took about 4 h and was carried out with vigorous agitation at room temperature (at or below 35 °C). During the addition the pH of the solution was maintained between 9 and 10. The slurry was cooled to room temperature, filtered and washed with demonized water until the pH of the filtrate was 7. After drying it at 373 K for 24 h, the solids were calcined at 723 K for 12 h. Here, the molar ratio of Mg to Al was fixed at 2. Thus, 10% (w/w) and 20% (w/w) CHT/HMS catalysts were prepared.

2.3. Reaction procedure and analysis

2.3.1. Aldol condensation of benzaldehyde with heptanal

Aldol condensation was studied in a 3.0 cm i.d. fully baffled mechanically agitated reactor of 50 cm^3 total capacity, which was equipped with a standard six-blade pitched – turbine impeller and a reflux condenser. The reactor was kept in an isothermal bath whose temperature could be maintained at the desired value by using a temperature indicator controller. Experiments were conducted under nitrogen atmosphere. Standard experiment was conducted with 0.05 mol benzaldehyde, 0.01 mol heptanal, and 0.1 g/cm^3 of catalyst based on total liquid volume, at 150 °C and 1200 rpm. A zero sample was drawn before commencement of agitation at 150 °C.

2.3.2. Analysis

Samples were withdrawn periodically and analyzed by GC (Chemito Model 8510), coupled with FID on a stainless steel column (3.25 mm × 2 m) packed with a liquid stationary phase of OV-17. The injector and detector temperatures were programmed from 100 °C to 300 °C with a ramp rate of 10 °C/min. Nitrogen was used as the carrier gas at a flow of 0.5 cm^3/s. Quantitative results were obtained through calibration by using synthetic mixtures of reactants and products. Products were confirmed by GC–MS.

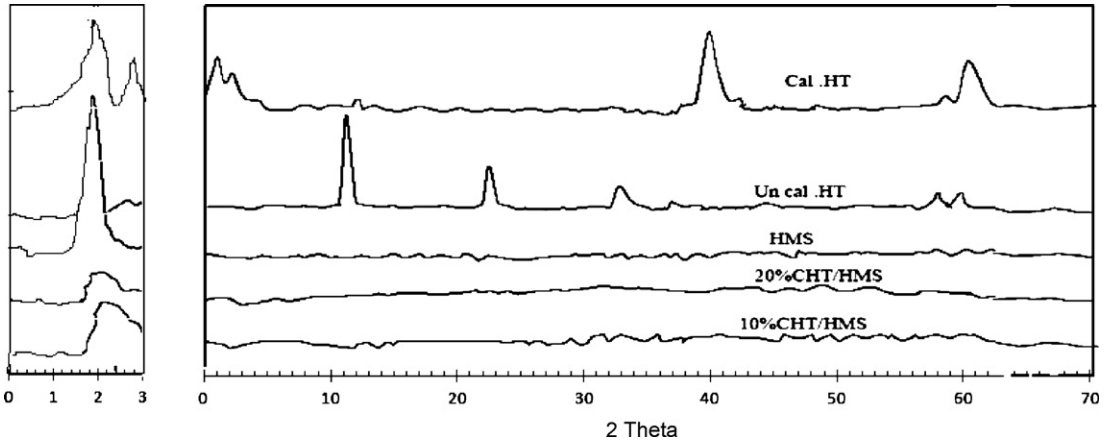

Fig. 1. X-ray diffractions patterns of synthesized materials.

3. Results and discussion

3.1. Catalyst characterization

3.1.1. X-ray diffraction

The X-ray diffraction (XRD) patterns of all synthesized materials were recorded (Fig. 1). The region between 2θ of 0–3° is properly expanded and it shows a strong reflection (1 0 0) at 2θ of 2.3. Calcined HMS exhibited a strong reflection (1 0 0) at about 2.3 corresponding to $d = 4$ nm and no peak is observed after 2-theta of 4.00. There is a strong peak at around 2.0° for HMS whose intensity is reduced in 10% and 20% HT/HMS. The UnCHT shows reflections (0 0 3), (0 0 6) and (0 1 2) for 2θ values of 11.4, 22.8 and 34.7, respectively (PCPDF card number 35-0965), indicating layered crystalline structure. These give a basal spacing decrease (d_{003}) and shift towards higher 2-theta values. On calcinations, the hydrotalcite structure was lost. CHT has a very broad, diffuse, and weak diffraction of magnesium oxide. The characteristic diffraction at 43 and 63° in CHT are attributed to mixed Mg–Al oxides and especially MgO (PCPDF card number 02-1207). On heating to 450 °C, UnCHT appears to lose its water and CO_2 to create vent holes in the crystal surface, which are not formed by exfoliation of metal layers. This fact is also supported by other observations such as a modest increase in surface area, retention of the crystal morphology and appearance of numerous fine pores in 20–40 Å sizes. No peak was observed in XRD patterns of both 10% and 20% w/w CHT/HMS samples, in the range of 10–70° 2-theta values. This can be attributed to the formation of nano-size particles of CHT inside the porous matrix of HMS. For low 2-theta values, a decrease in reflections is observed in the XRD pattern of both 10% and 20% CHT/HMS, which can be attributed to partial destruction of walls of HMS or blocking of some pores by CHT formed in situ.

3.1.2. TG–DTA

Fig. 2 shows the TG–DTA curves of all synthesized materials. Because HMS had been calcined at 650 °C for 4 h, there is almost no weight loss in the TG curve. HMS was prepared from an organic silica source by templating and there is carbonization and oxidation of the organic material, there is loss of the organic mass. The structure is reasonably stable when calcined at 650 °C and any remaining matter is totally removed from the material up to 800 °C.

Two endothermic peaks are observed in DTA and almost 40% weight loss peak is observed in TG of the UnCHT. The first weight loss observed below 200 °C is due to the loss of interlayer water and physically absorbed moisture. Next loss of weight, above 300 °C, is due to the loss of CO_2 from interlayer carbonate anions and also hydroxy groups from the brucite-like ($Mg(OH)_2$) layers [41]. The hydrotalcite is $Mg_6Al_2(OH)_{16}CO_3{\cdot}4H_2O$ and on calcination it gives $Mg_6Al_2O_8(OH)_2$. Hydrotalcites are stable up to 400 °C. At 200 °C, water molecules are lost and anhydrous hydrotalcite is obtained. At higher temperatures, CO_3^{2-} (carbonate) is removed and solids are partially hydroxylated; $Mg_6Al_2O_8(OH)_2$ is formed. If calcined at temperatures higher than 450 °C and up to 900 °C, MgO (periclase) and the spinel $MgAl_2O_4$ are irreversibly obtained. But, if calcined at around 500 °C, $Mg_6Al_2O_8(OH)_2$ is formed and, in the presence of water and carbonates, the original hydrotalcite is recovered [42,43].

A weight loss of 12% is observed for CHT. Because CHT was calcined at 450 °C for 12 h, only one endothermic peak is observed, which is due to the loss of physically absorbed moisture. Small endothermic peaks for 10 and 20% (w/w) CHT/HMS are noticed due to dehydration. When the CHT content on HMS is increased from, 10% to 20% (w/w), the weight loss increased correspondingly. The weight loss was due to the loss of physically adsorbed moisture and dehydration. The loss in weight per unit mass of HMS of 10% and 20% CHT/HMS was the same.

From these results, it is deduced that there was no impurity in both 10% and 20% (w/w) CHT/HMS catalysts.

3.1.3. FT-IR spectra

FT-IR spectra (Shimadzu) of HMS (Fig. 3) shows absorption at 1092 cm^{-1} and its shoulders may be assigned to the asymmetric stretching of Si–O–Si [44]. The peaks at around 470 and 810 cm^{-1} are also given by internal bands of SiO_4 tetrahedra, whereas the broad band at ~3400 cm^{-1} is associated with hydrogen-bonded silanol group vibration. Some very small peaks are observed at 1400–1500 cm^{-1}, arising from aliphatic C—H stretching vibrations. The peaks at 2800–3000 cm^{-1} arise from C—H bending, which indicate that the template may not have been removed completely from HMS even though it was calcined at 450 °C.

In the case of CHT, a broad absorption band seen at 3459 cm^{-1}, is attributed to the stretching of hydrogen-bonded hydroxyl group and water molecules; the corresponding deformation mode (dHOH) has appeared at ~1630 cm^{-1} [45,46]. The absorption bands n3, n2 and n4, due to stretching vibration of interlayer CO_3^{2-} ions were observed at ~1368, 657 and 787 cm^{-1}, respectively and those at 410 and 430 cm^{-1} are related to cation-oxygen vibrations in UnCHT. Because of calcination at 450 °C, the intensities of all bands for CHT are greatly reduced. The presence of broadened absorption band at ~3450 cm^{-1} indicates that a sizeable amount of hydroxyl groups are still present in the brucite-layer. Also, the absorption band due to n3 mode splits into two lines indicating that the symmetric feature of CO_3^{2-} site is lost in the calcined sample. Small broad band at 1638 cm^{-1} may be assigned to the water-bending bond between the layers. This may be due to physically adsorbed

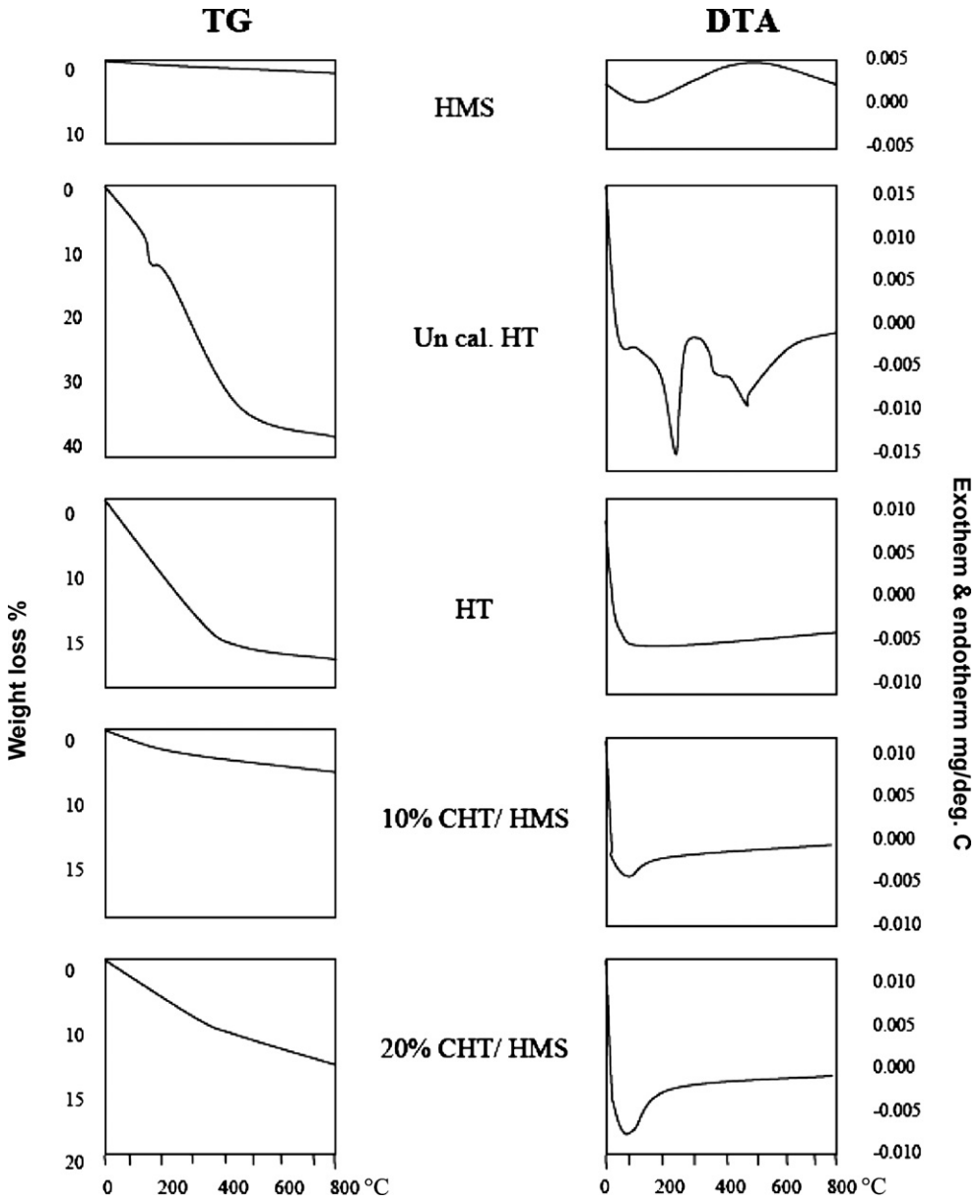

Fig. 2. TG–DTA curves of synthesized materials.

water from atmosphere in small amount. All remaining peaks for 10% and 20% (w/w) CHT/HMS samples show similarity with those of HT and HMS samples, but with a little difference.

3.1.4. Surface area and pore size analysis

The textural characterization of HMS, 10% and 20% (w/w) CHT/HMS were determined by nitrogen BET surface area measurements (Micromeritics ASAP 2010). The pore size distribution was calculated from the adsorption curve by BJH method. HMS, 10 and 20% (w/w) CHT/HMS display characteristic type IV adsorption isotherms with well-defined steps in N_2 adsorption and desorption isotherms. There is a hysteresis in the adsorption isotherm at relative pressure (p/p_0) in the range of 0.40–0.8. Physical properties of HMS, 10% and 20% (w/w) CHT/HMS catalysts are given in Table 1. In both 10% and 20% (w/w) CHT/HMS samples, the BJH average diameter is centered on 38 Å without any broadening and it displays fairly uniform pore size distribution. The average pore diameter of HMS is 40 Å. As the loading of CHT on HMS is increased from 10% to 20% (w/w), the surface area of the material is decreased. The reduction in the BET surface area and pore volumes of CHT/HMS with reference to HMS is more remarkable in comparison with their respective pore sizes. This indicates that nano-particles of magnesium and aluminum mixed oxides are generated on HMS on calcination and some large particles could have blocked a few pore junctions thereby reducing accessibility of some channels of the support, for the probe molecule. During the synthesis of CHT/HMS, growth of crystalline magnesium–aluminum oxides is very unlikely, as evidenced by the XRD analysis and BET surface area measurement. They indicate that the characteristic hexagonal structure of the HMS and mesoporosity are not disturbed upon

Table 1
Physical properties of catalysts.

Physical property	HMS	10% (w/w) CHT/HMS	20% (w/w) CHT/HMS
BET surface area (m^2/g)	1148	571	531
BJH pore volume (cm^3/g)	0.93	0.91	0.73
BJH average diameter (4 V/A) Å	40	38.20	38.10

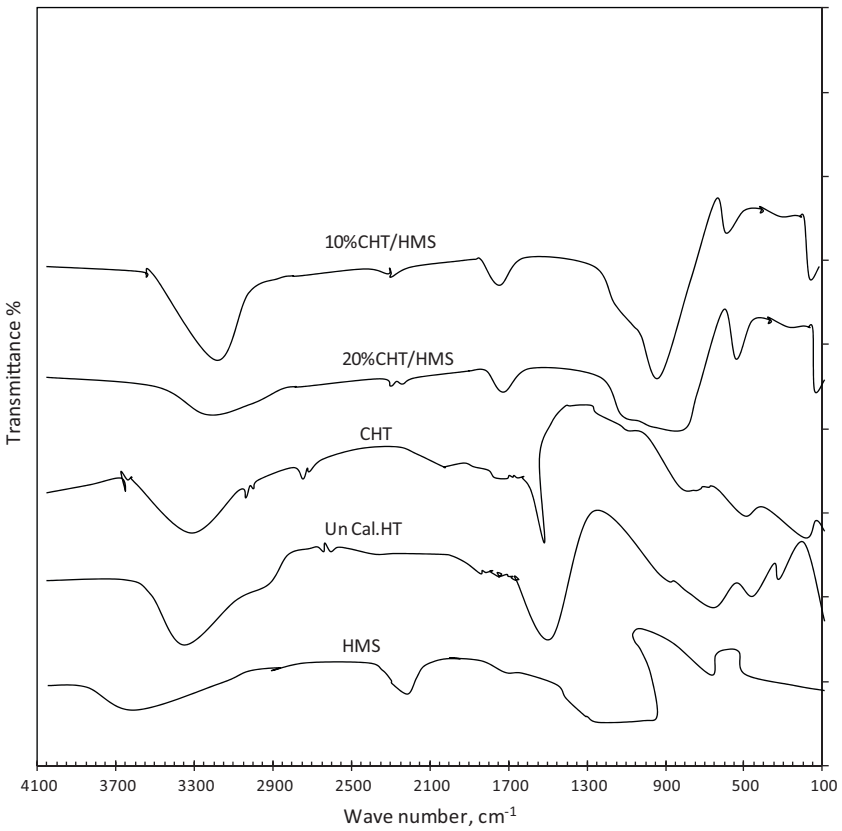

Fig. 3. FT-IR spectra of synthesized materials.

loading with CHT to make 10% and 20% (w/w) CHT/HMS. This also shows stability of the framework. This explanation is in accordance with IUPAC classification [47].

3.1.5. Transmission electron microscopy (TEM) and energy-dispersive X-ray spectroscopy (EDXS)

TEM images for 20% (w/w) CHT/HMS catalysts are shown in Fig. 4. The micrographs show that Mg–Al oxides are uniformly dispersed on HMS and the CHT loading does not disturb the hexagonal structure of HMS. It also confirms that CHT particles are located on surface of HMS. The EDXS analysis (KEVEX X-ray spectrometer) shows the incorporation of CHT in HMS (Table 2).

3.2. Aldol condensation

The activity and stability of the prepared catalysts were tested in the aldol condensation of benzaldehyde with helptaldehyde with CHT, 10 and 20% (w/w) CHT/HMS were evaluated at 150 °C. The main product was jasminaldehyde with the side product (E)-2-*n*-pentyl-2-*n*-nonenal, which is a self-condensation product of heptanal (Scheme 1). No other by-product was detected in the reaction mixture.

Table 2
EDXS of HMS and 20% (w/w) CHT/HMS.

Element	Weight %	Atomic %
(a) HMS		
O	54.49	67.76
Si	45.54	32.24
Total	100.00	100.00
(b) 20% (w/w) CHT/HMS		
O	49.08	62.34
Mg	6.11	5.11
Al	4.08	3.07
Si	40.74	29.48
Total	100.00	100.00

3.2.1. Reaction mechanism

Mg^{2+} ions are partly replaced by Al^{3+} ions in HT, which leads to positively charged cation layers. Charge-balancing anions (usually CO_3^{2-}) and water molecules are situated in the interlayers between the stacked brucite-like cation layers. The as-synthesized HT structure displays no catalytic activity in aldol condensation. However, a controlled heat treatment to 450 °C is needed to form an Mg(Al)O mixed oxide phase which catalyzes various gas-phase condensation reactions [41,44–46,48]. For HT, Brønsted base sites (OH^- groups) are the main basic sites. However, Lewis (O^{2-} anions) and Brønsted base sites are present on the surface of CHT samples. Lewis base sites on the CHT samples are predominant with respect to their amount and the strength in comparison with Brønsted base sites [46,48–50]. It suggests that OH^- groups enhance catalytic activity in CHT; however, they are not the sole source of the enhancement.

A possible mechanism based on the synergistic cooperation of the weak acid sites with the basic sites, adjacent to one another, is proposed as shown in Scheme 2 with reference to CHT/HMS. Initially, heptanal is exclusively activated by deprotonation of the α-C atom by the base site on the surface of the catalyst to produce a carbanion. This leads to the formation of an enolate. At the same time, benzaldehyde via its O atom is bonded to the surface of the adjacent Lewis acid site (Al) which is a weak site. The role of the Lewis acid sites is to interact with the C=O group of the benzaldehyde producing a polarization of that group and increasing the positive charge on that α-carbon atom. It would render the α-carbon of benzaldehyde more susceptible for attack by the enolate anion of heptanal formed on the adjacent strong base site. It produces an intermediate alkoxide. Subsequently, the

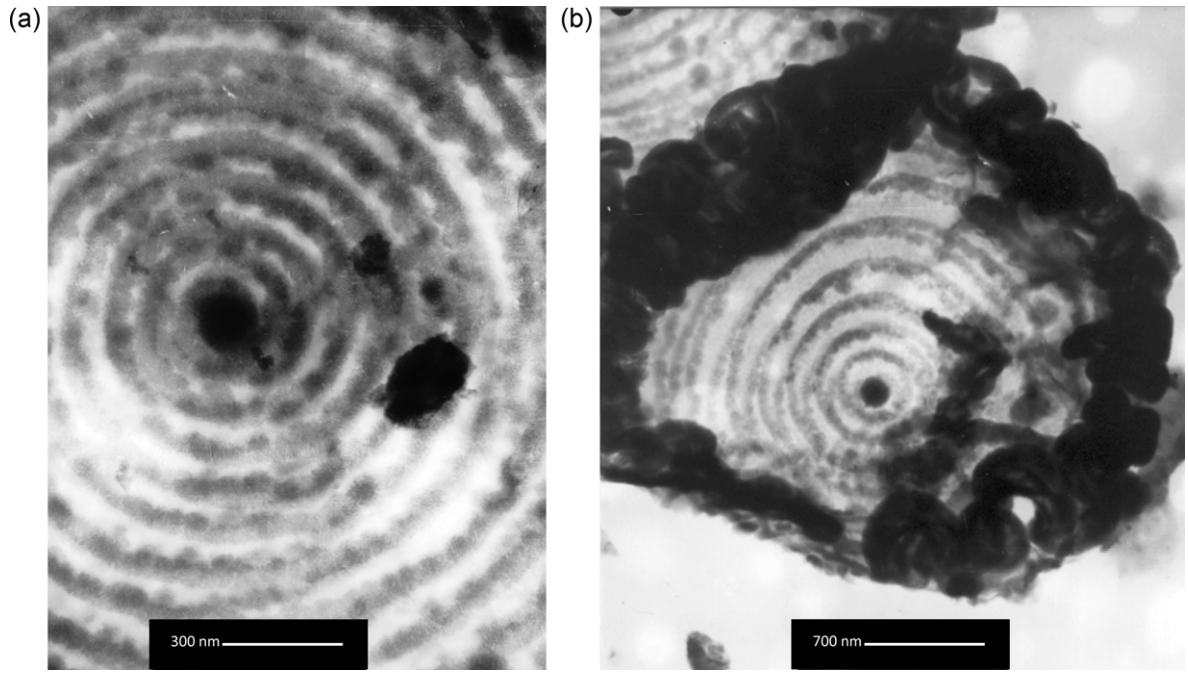

Fig. 4. TEM images of (a) 10% (w/w) CHT/HMS and (b) 20% (w/w) CHT/HMS.

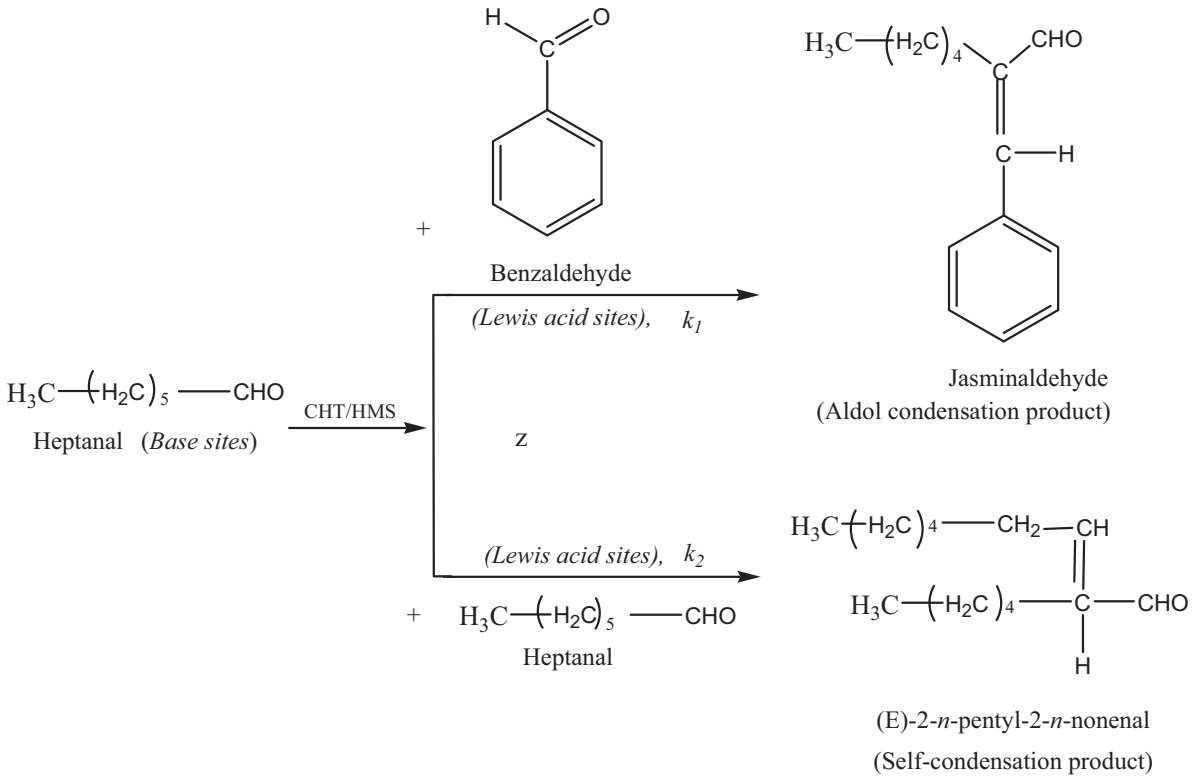

Scheme 1. Aldol condensation of benzaldehyde and heptanal.

alkoxide deprotonates a water molecule, and thus creates a hydroxide and a β-hydroxyaldehyde or aldol product. Basic and acidic sites located close to each other cooperate to yield high activities. Thus, jasminaldehyde is produced. Climent et al. also observed a cooperative effect between weak acid and base sites in aldol condensations on solid acid catalysts [49]. Activated layered double hydroxides (LDHs) with high crystallinity were obtained by calcination/rehydration of LDH precursors, which were synthesized by urea decomposition [50]. LDHs were found to have higher catalytic activity in acetone self-condensation. An acid–base catalytic mechanism has been proposed to interpret the catalytic behavior based on the fact that acid–base hydroxyl group pairs on the activated LDH surface have a separation of 0.31 nm. It has been proposed that the active sites are mainly located on the ordered array of hydroxyl sites on the basal surfaces rather than on the edges [50].

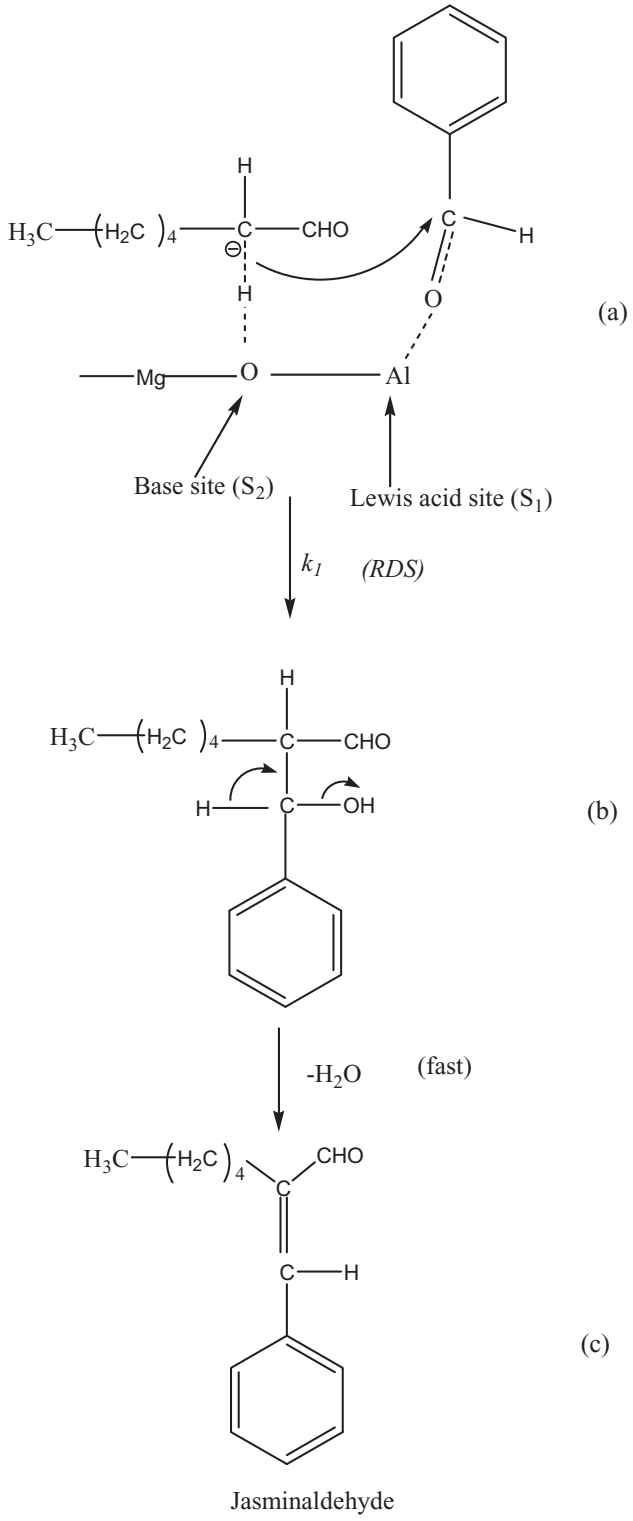

Scheme 2. Reaction mechanism for aldol condensation of benzaldehyde with heptanal.

Scheme 3 shows a mechanism for the self-condensation of heptanal based on the bi-functional CHT/HMS, in which heptanal molecules adsorbed on two adjacent acid–base sites produce the self-condensation product. This would suggest that benzaldehyde should be used in high concentration over heptanal to reduce adsorption of heptanal on Lewis acid sites. Heptanal, being an aliphatic aldehyde, is more reactive than benzaldehyde. Therefore the self-condensation of heptanal is a parallel reaction which

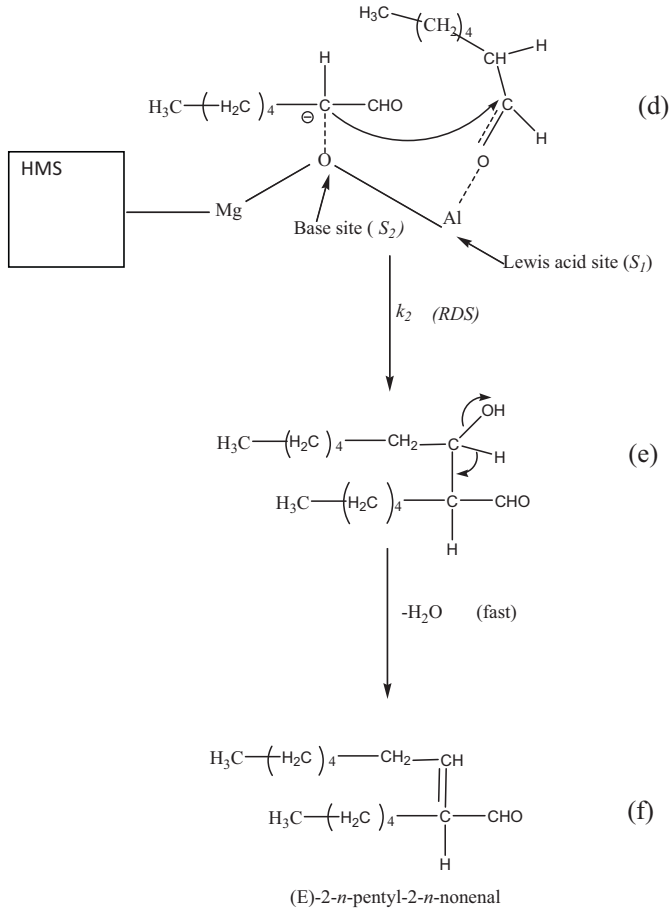

Scheme 3. Self-condensation of heptanal to produce (E)-2-n-pentyl-2-*n*-nonenal.

severely reduces the yield to jasminaldehyde. Indeed, heptanal competes for the acidic site along with benzaldehyde. The foregoing hypothesis was tested by studying the effects of different variables on conversion and rates of reaction.

3.2.2. Kinetic model

Based on the above mechanism, the overall reaction is represented by the following two parallel reactions of heptanal (Scheme 1):

$$A + B \xrightarrow{k_1} C + W \quad \text{(aldol condensation)} \tag{1}$$

$$2B \xrightarrow{k_2} D + W \quad \text{(self-condensation of heptanal)} \tag{2}$$

where A, B, C, D and W are benzaldehyde, heptanal, jasminaldehyde, (E)-2-*n*-pentyl-2-*n*-nonenal and water, respectively.

In the absence of any external mass transfer and intra-particle diffusion resistances, which have been discussed separately, a Langmuir–Hinshelwood–Hougen–Watson model is developed for a bi-functional catalyst. Sites S_1 and S_2 are uniformly distributed on the pore walls of HMS. Benzaldehyde (A) gets adsorbed on to the Lewis acid site (S_1) and heptanal on the base site (S_2) to produce the chemisorbed species AS_1 and BS_2:

$$A + S_1 \overset{K_{A_1}}{\rightleftarrows} AS_1 \tag{1'}$$

$$B + S_2 \overset{K_{B_2}}{\rightleftarrows} BS_2 \tag{2'}$$

These two chemisorbed species participate in the aldol reaction on the surface to produce jasminaldehyde (C) and water (W) as given below.

$$BS_2 + AS_1 \xrightarrow{k_{SR}} CS_2 + WS_1 \quad (3)$$

The chemisorbed products are desorbed in the pore space according to the following:

$$CS_2 \overset{1/K_{C_2}}{\rightleftarrows} C + S_2 \quad (4)$$

$$WS_1 \overset{1/K_{W_1}}{\rightleftarrows} W + S_1 \quad (5)$$

Heptanal also competes for acidic sites (S1):

$$B + S_1 \overset{K_{B_1}}{\rightleftarrows} BS_1 \quad (6)$$

The self-condensation takes place due to the reaction of heptanal adsorbed on two adjacent but different sites (S_1 and S_2) as given below (Scheme 3):

$$BS_2 + BS_1 \xrightarrow{k_{SR_2}} DS_2 + WS_1 \quad (7)$$

The chemisorbed products are desorbed in the pore space according to the following:

$$DS_2 \overset{1/K_{D_2}}{\rightleftarrows} D + S_2 \quad (8)$$

It is assumed that there is no reaction of heptanal molecules adsorbed on two adjacent basic sites.

The total site concentration (C_T), in moles per unit mass of catalyst is given below:

$$C_T = C_{T-S_1} + C_{T-S_2} \quad (9)$$

where

$$C_{T-S_1} = C_{VS_1} + C_{AS_1} + C_{BS_1} + C_{WS_1} \quad (10)$$

$$C_{T-S_2} = C_{VS_2} + C_{BS_2} + C_{CS_2} + C_{DS_2} \quad (11)$$

Writing in terms of adsorption equilibrium constants for each species on the corresponding site, the concentration of the vacant sites S_1 and S_2 are obtained as follows:

$$C_{VS_1} = \frac{C_{T-S_1}}{1 + K_{A_1}C_A + K_{B_1}C_B + K_{W_1}C_W} \quad (12)$$

$$C_{VS_2} = \frac{C_{T-S_2}}{1 + K_{B_2}C_B + K_{C_2}C_C + K_{D_2}C_D} \quad (13)$$

The rate of formation of jasminaldehyde (r_C) is given by:

$$r_C = \frac{dC_C}{dt} = k_{SR_1}C_{BS_2}C_{AS_1} = k_{SR_1}K_{B_2}C_BC_{VS_2}K_{A_1}C_AC_{VS_1} \quad (14)$$

Eq. (14) on substitution for concentration of vacant sites leads to:

$$r_C = \frac{k_{SR_1}K_{B_2}K_{A_1}C_{T-S_1}C_{T-S_2}C_AC_B}{(1 + K_{A_1}C_A + K_{B_1}C_B + K_{W_1}C_W)(1 + K_{B_2}C_B + K_{C_2}C_C + K_{D_2}C_D)} \quad (15)$$

In terms of catalyst loading w (g/cm^3 of total liquid volume), Eq. (14) becomes:

$$r_C = \frac{k_{SR_1}K_{B_2}K_{A_1}wC_AC_B}{(1 + K_{A_1}C_A + K_{B_1}C_B + K_{W_1}C_W)(1 + K_{B_2}C_B + K_{C_2}C_C + K_{D_2}C_D)} \quad (16)$$

Similarly, the rate of formation of the self-condensation product (r_D) is:

$$r_D = \frac{dC_D}{dt} = \frac{k_{SR_2}K_{B_2}K_{B_1}wC_B^2}{(1 + K_{A_1}C_A + K_{B_1}C_B + K_{W_1}C_W)(1 + K_{B_2}C_B + K_{C_2}C_C + K_{D_2}C_D)} \quad (17)$$

Since no other by-product is formed by reaction of benzaldehyde, the rate of reaction of benzaldehyde ($-r_A$) is given by:

$$-r_A = \frac{-dC_A}{dt} = r_C = \frac{k_{SR_1}K_{B_2}K_{A_1}wC_AC_B}{(1 + K_{A_1}C_A + K_{B_1}C_B + K_{W_1}C_W)(1 + K_{B_2}C_B + K_{C_2}C_C + K_{D_2}C_D)} \quad (18)$$

If the adsorption of all species is weak then, all terms in the denominator in Eq. (18) are equated to one. Preliminary analysis of the data suggested that there was weak adsorption of the reactants, and the Langmuir–Hinshelwood–Hougen–Watson model reduces to a power-law model as follows:

$$r_C = -r_A = \frac{-dC_A}{dt} = k_{SR_1}K_{B_2}K_{A_1}wC_AC_B = k_1wC_AC_B = k_1'wC_B \quad (19)$$

Since, high mole ratio of benzaldehyde to heptanal was used,

$$C_A \gg C_B, \quad k_1C_A \approx k_1C_{A0} = k_1' \cong a \quad \text{pseudo-constant} \quad (20)$$

Now the rate of reaction of heptanal ($-r_B$) by two parallel reactions can be written as:

$$-r_B = \frac{-dC_B}{dt} = k_{SR_1}K_{B_2}K_{A_1}wC_AC_B + k_{SR_2}K_{B_2}K_{B_1}wC_B^2 = kwC_AC_B + k_2wC_B^2 = k_1'wC_B + k_2wC_B^2 \quad (21)$$

The selectivity ratio of C over D ($S_{C/D}$) is defined by the ratio of rate of formation of C over that of D and is given by:

The formation of jasminaldehyde:

$$r_C = \frac{dC_C}{dt} = k_{SR_1}K_{B_2}K_{A_1}wC_AC_B$$

$$r_D = \frac{dC_D}{dt} = k_{SR_2}K_{B_2}K_{B_1}wC_B^2$$

$$S_{C/D} = \frac{r_C}{r_D} = \frac{dC_C/dt}{dC_D/dt} = \frac{dC_C}{dC_D} = \frac{k_{SR_1}K_{A_1}C_A}{k_{SR_2}K_{B_1}C_B} \quad (22)$$

Eq. (22) shows that in order to increase the selectivity to jasminaldehyde (C), the following conditions should be obeyed: (i) the adsorption constant (K_{B_1}) of heptanal on Lewis acid sites should be low, (ii) the rate constant for self-condensation (k_{SR_2}) should be very small, (iii) heptanal concentration (C_B) should be low, (iv) the concentration of benzaldehyde should be high, and (V) the adsorption constant for benzaldehyde on Lewis acid site (K_{A_1}) should be high, or the term $K_{A_1}C_A$ should be kept high, Further if the activation energy for the aldol condensation is greater than that for self-condensation of helptanal, then an increase in temperature will increase selectivity.

The selectivity of C (Y) is also defined by the rate of formation of C with reference to the rate of reaction of B:

$$Y = \frac{r_C}{r_C + r_D} = \frac{r_C}{-r_B} = \frac{dC_C/dt}{-dC_B/dt} = \frac{k_{SR_1}K_{A_1}C_A}{k_{SR_1}K_{A_1}C_A + k_{SR_2}K_{B_1}C_B} = \frac{1}{1 + (k_{SR_2}K_{B_1}C_B)/(k_{SR_1}K_{A_1}C_A)} \quad (23)$$

From Eq. (21) for weak adsorption of all species:

$$\frac{-dC_B}{dt} = k_1C_AC_B + k_2C_B^2 \quad (24)$$

Since $C_A \gg C_B$, Eq. (1) becomes pseudo-1st order with respect to B

$$-\frac{dC_B}{dt} = k_1'C_B + k_2C_B^2 \quad (25)$$

Table 3
Comparison of CHT catalysts.[a]

No.	Catalyst	Conversion of heptanal (%)	Selectivity to jasminaldehyde $Y_{C/B}$ (%)	Selectivity ratio ($S_{C/D}$=)
1	CHT	95	59	1.44
2	10% (w/w) CHT/HMS	65	80	4.00
3	20% (w/w) CHT/HMS	82	86	6.14

[a] Benzaldehyde to heptanal mol ratio: 5:1, catalyst loading: 0.1 g/cm^3, temperature: 150 °C, and time: 4 h.

Where

$$k_1' = k_1 C_{A0} \tag{26}$$

Separating the variables, the following is obtained:

$$-\frac{dC_B}{C_B(k_1' + k_2 C_B)} = dt \tag{27}$$

$$\frac{-1}{k_1'}\left[\frac{1}{C_B} - \frac{k_2}{k_1' + k_2 C_B}\right] dC_B = dt \tag{28}$$

$$-\left[\ln C_B - \frac{k_2}{k_1'}\ln(k_1' + k_2 C_B)\right]_{C_{B0}}^{C_B} = k_1'[t]_0^t \tag{29}$$

$$\left[\ln\left(\frac{k_1' + k_2 C_B}{C_B}\right)\right]_{C_{B0}}^{C_B} = k_1' t \tag{30}$$

$$\ln\left(\frac{(k_1' + k_2 C_B)w}{C_B}\right) - \ln\left(\frac{(k_1' + k_2 C_{B0})w}{C_{B0}}\right) = k_1' wt \tag{31}$$

When the catalyst loading (w) is constant, Eq. (31) can be rewritten as:

$$\ln\left(\frac{k_1'' + k_2' C_B}{C_B}\right) = \ln\left(\frac{k_1'' + k_2' C_{B0}}{C_{B0}}\right) + k_1'' t \tag{32}$$

Where

$$k_1'' = k_1' w \text{ and } k_2' = k_2 w \tag{33}$$

Thus, a plot of $\ln(k_1'' + k_2' C_B/C_B)$ against t can be made to get a straight line with an intercept of $\ln(k_1'' + k_2' C_{B0}/C_{B0})$ and slope of k_1'' for a fixed value of w. This will be discussed later.

3.2.3. Catalyst evaluation

The activities and selectivities of unsupported CHT, 10% and 20% (w/w) CHT/HMS are given in Table 3. The conversion and selectivity obtained with CHT alone are 95% and 59%, respectively, when the same amount of catalyst is used. On the contrary 20% (w/w) CHT/HMS gives 82% conversion of heptanal with 86% selectivity to jasminaldehyde ($S_{C/D}$ = 6.14) in 4 h for a benzaldehyde to heptanal mole ratio of 5:1 at 150 °C at a catalyst loading (w) of 0.1 g/cm^3 based on total liquid volume. Thus, 20% (w/w) CHT/HMS is a better catalyst. The ordered mesoporosity of CHT/HMS as well as low value of the constant $k_{SR_2}K_{B_1}$ and lower concentration of heptanal are responsible for suppression of the by-product formation, under operating conditions. That is – the adsorption of heptanal on acidic sites must be reduced.

3.2.4. Catalyst reusability

Reusability of the catalyst was tested by conducting two separate experiments (Table 4). At the end of the reaction, the catalyst was filtered and refluxed with 50 cm^3 of solvent (1:1 ratio of ethanol and methanol) for 30 min in order to remove any adsorbed material from pores of catalyst. It was dried at 120 °C and used in the next experiment. There was a small decrease in conversion of heptanal without any change in selectivity of jasminaldehyde. There was no make-up when the catalyst was reused. There were losses during filtration and drying and thus about 5% of catalyst was lost.

Table 4
Effect of reusability of 20% (w/w) CHT/HMS on aldol-condensation of benzaldehyde and heptanal.[a]

Reusability	Conversion of heptanal, %	Selectivity to jasminaldehyde, %
Fresh	82	86
1st	80.5	83
2nd	80	82

[a] Conditions: benzaldehyde:heptanal: 5:1, catalyst loading: 0.1 g/cm^3, temperature: 150 °C, and speed of agitation: 1200 rpm.

When experiments were conducted with used catalyst where the make-up of lost catalyst was made to get the same results. Thus, the catalyst is stable and reusable.

3.2.5. Effect of speed of agitation

In all reactions, benzaldehyde was taken in far molar excess (5:1) over heptanal to reduce the by-product formation and drive the equilibrium towards the product. To determine the influence of external resistance to mass transfer of the reactants to the catalyst surface, the speed of agitation was varied from 700 to 1400 rpm (Fig. 5). The speed of agitation had no effect of conversion and selectivity beyond 1200 rpm and thus there was no limitation of external mass transfer of heptanal from bulk liquid phase to the outer surface of the catalyst beyond 1200 rpm speed. Further, since heptanal (B) was the limiting reactant, a theoretical calculation was done to establish that the resistance to mass transfer was negligible in comparison with the overall resistance as given below. The solid-liquid mass transfer coefficient was obtained from the limiting Sherowood number (=2). The observed rate of reaction was taken as the initial rate of reaction:

$$\frac{1}{k_{SL-B} a_p C_{B0}} \ll \frac{1}{r_{obs}} \tag{27'}$$

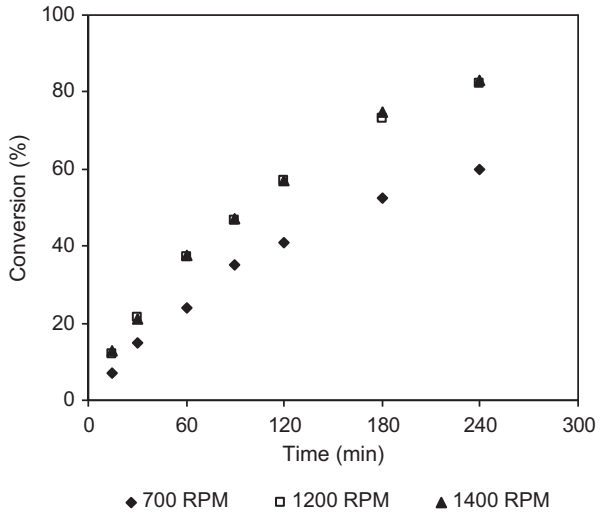

Fig. 5. Effect of speed of agitation on conversion of heptanal: temperature: 150 °C, benzaldehyde:heptanal: 5:1 (mol), 20% (w/w) CHT/HMS catalyst loading: 0.1 g/cm^3.

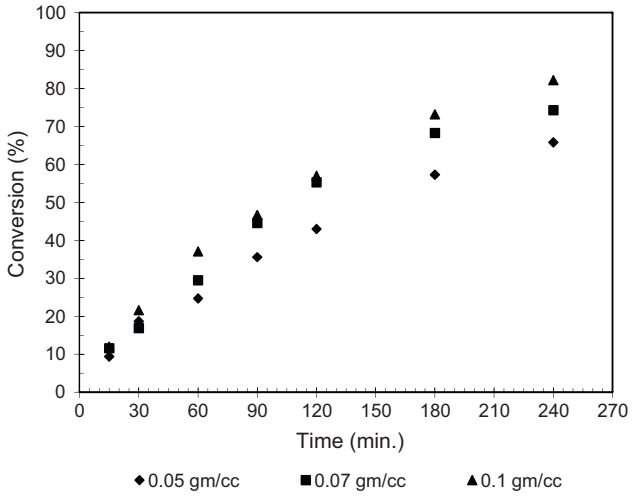

Fig. 6. Effect of catalyst loading on conversion of heptanal: temperature: 150 °C, speed of agitation: 1200 rpm, benzaldehyde:heptanal: 5:1 (mol), catalyst: 20% CHT/HMS.

So, further experiments were conducted at 1200 rpm. This inequality shows that the concentration of heptanal on the outer surface of the catalyst was the same as that in the bulk liquid phase.

3.2.6. Effect of catalyst loading

In the absence of mass transfer resistance, the rate of reaction is directly proportional to catalyst loading based on the entire volume of the liquid phase. The catalyst loading was varied from 0.05 to 0.1 g/cm^3 on the basis of the total volume of the reaction mixture (Fig. 6). As the catalyst loading was increased the conversion of heptanal increased, which was due to proportional increase in the number of active sites. There was no change in selectivity to jasminaldehyde.

The Wiesz–Prater modulus [51] was calculated as 3.1×10^{-3} and thus there was no intra-particle resistance.

3.2.7. Effect of mole ratio of heptanal to benzaldehyde

The mole ratio of heptanal to benzaldehyde was varied from 1:2 to 1:10. With an increase in mole ratio, the conversion of heptanal increased (Fig. 7(a)) and also the selectivity to jasminaldehyde increased (Fig. 7(b)). At lower mole ratios, the concentration of heptanal is more and hence its rate of reaction is higher; it competes with benzaldehyde for adsorption on the acid sites (S_1). The protonation as well as subsequent activation of heptanal carbonyl group takes place on the acidic sites, leading to extensive self-condensation with another heptanal molecule, which is already in the vicinity, adsorbed on the basic sites (S_2). Hence the selectivity to jasminaldehyde decreases. This happens up to a mole ratio of 1:5 which corresponds to initial moles of for initial concentrations of heptanal ($C_{B_0} = 0.00154$) and benzaldehyde ($C_{A_0} = 0.0074$). When the mole ratio is changed from 1:5 to 1:10, there is no change is conversion; however, the selectivity to jasminaldehyde increases from 86% to 92%. Adding more quantity of benzaldehyde is not advisable since increases the dilution and increases the reactor volume considerably. So, it was concluded that a mole ratio of 1:5 is an optimum for reducing the self-condensation of heptanal.

3.2.8. Self-condensation of heptanal

The self-condensation of heptanal was studied independently at three different temperatures in the range of 130–150 °C by using

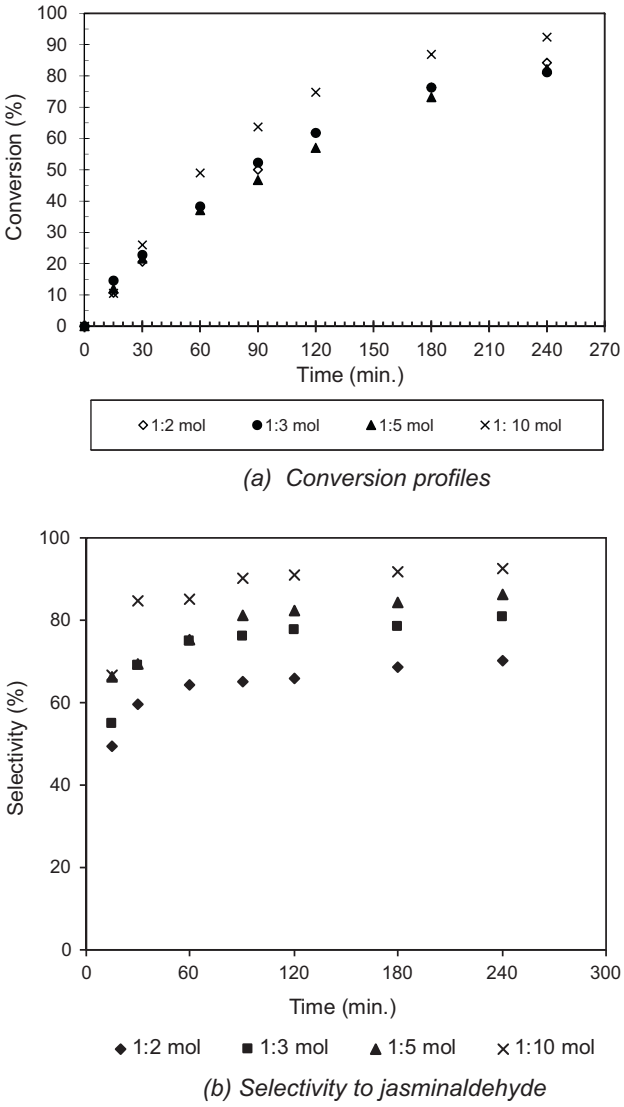

Fig. 7. Effect of mole ratio of heptanal to benzaldehyde on conversion of heptanal and selectivity to jasminaldehyde: (a) conversion profiles and (b) selectivity to jasminaldehyde. Catalyst loading: 0.1 g/cm^3, temperature: 150 °C, speed of agitation: 1200 rpm, and catalyst: 20% CHT/HMS.

the same catalyst loading and without any solvent. The rate of self-condensation of heptanal is given by:

$$-r_{B_2} = \frac{-dC_B}{dt} = k_{SR_2} K_{B_2} K_{B_1} w C_B^2 = k_2 w C_B^2 = k_2' C_B^2 \quad (28')$$

The above equation can be written in terms of fractional conversion of heptanal (X_B) and integrated to get the following:

$$\frac{X_B}{1 - X_B} = k_2' C_{B0} t = k_2 w C_{B0} t \quad (29')$$

Thus, plots are made of $X_B/1 - X_B$ versus time in Fig. 8 to validate the above model. The slopes so obtained were used to calculate the activation energy for self-condensation as 19.75 kcal/mol (Fig. 9). This value suggests that the reaction is intrinsically kinetically controlled.

3.2.9. Effect of temperature on aldol condensation

Since this is a complex reaction network, temperature not only affects the reaction rate but also alters the selectivity, provided the activation energies of the competing reactions are different. The effect of temperature on conversion of heptanal in aldol

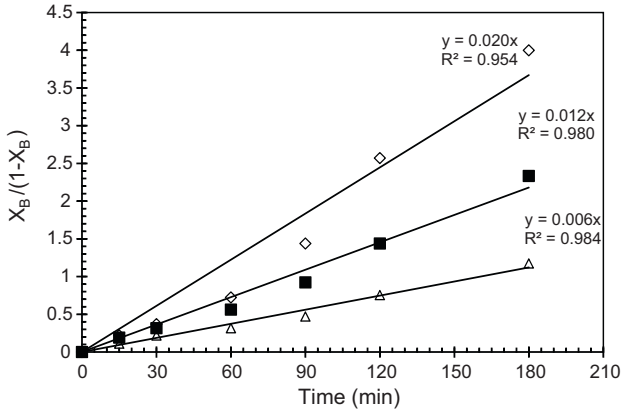

Fig. 8. Kinetic plot: XB/(1 – XB) versus time for self-condensation of heptanal.

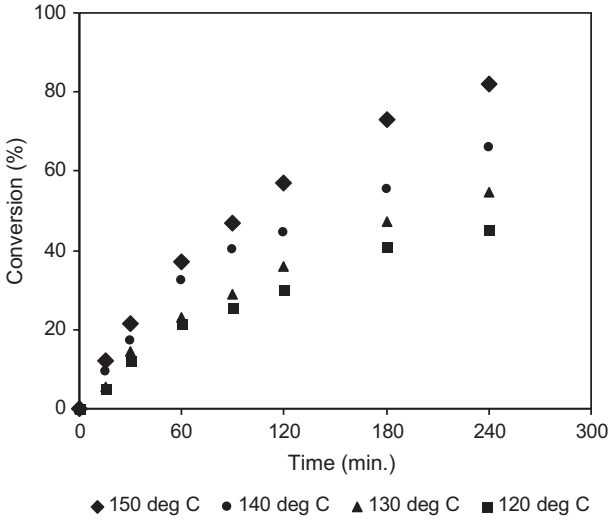

Fig. 10. Effect of temperature on aldol condensation of benzaldehyde with heptanal. Catalyst loading: 0.1 g/cm^3, speed of agitation: 1200 rpm, benzaldehyde:heptanal: 5:1 (mol).

condensation with benzaldehyde was studied in the range of 120–150 °C under otherwise similar conditions (Fig. 10). The conversion increased substantially with increasing temperature up to 150 °C. This observation also supported the earlier observations that the reaction was free from all mass transfer and intra-particle diffusion effects. As the temperature was increased, it was found that the selectivity to jasminaldehyde had decreased.

The selectivity ratio $S_{C/D}$ should be examined as given below:

$$S_{C/D} = \frac{r_C}{r_D} = \frac{dC_C}{dC_D} = \frac{k_{SR_1} K_{A_1} C_A}{k_{SR_2} K_{B_1} C_B} = \frac{A_{f1}}{A_{f2}} \exp\left(\frac{E_2 - E_1}{RT}\right) \frac{K_{A_1}}{K_{B_1}} \qquad (30')$$

The reaction rate constants k_{SR_1} and k_{SR_2} are strong function of temperature. The activation energy for self-condensation (E_2) should be lower than that for aldol condensation (E_1), then higher temperature will lead to increased selectivity. If the converse is true, then lower temperature will be beneficial. The values of pre-exponential factors and adsorption constants in Eq. (30) will be of the same order of magnitude. The selectivities at various temperatures are given in Table 5. Since the selectivity decreased with temperature, the activation energy E_1 appeared to be lower. Thus, the model was fitted as given below.

3.2.10. Evaluation of rate constants for aldol condensation

The following approaches were used to validate the model:

(a) Guessing values of rate constants and fitting Eq. (25).
(b) Using rate constant of self-condensation reaction obtained independently for initial guess and calculating the rate constant for aldol-condensation.
(c) The initial rate data for the reaction would give only the rate constant for aldol condensation within experimental error (since $k_1 > k_2$).

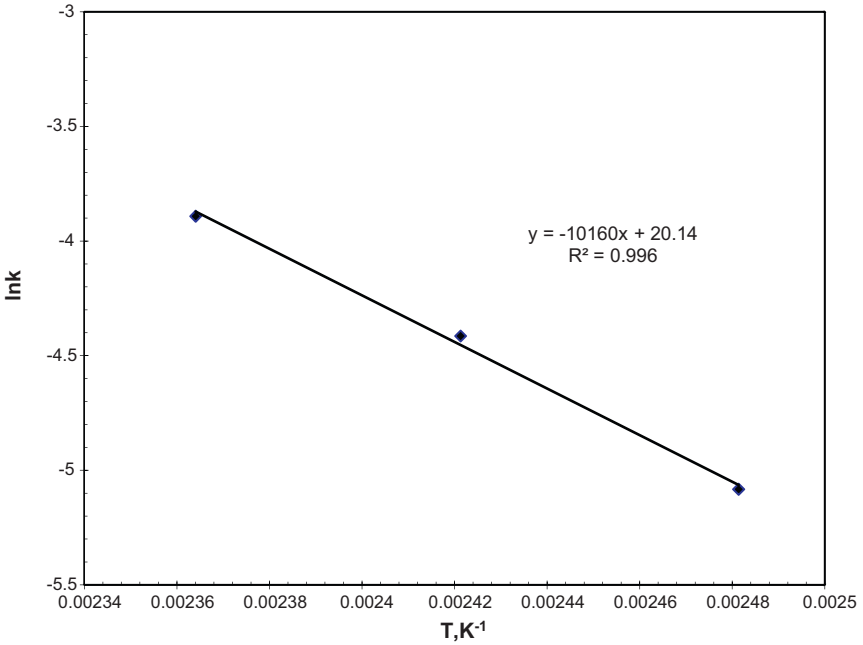

Fig. 9. Arrhenius plot for self-condensation of heptanal. Effect of temperature on selectivity of jasminaldehyde. Catalyst loading: 0.1 g/cm^3, speed of agitation: 1200 rpm, and benzaldehyde:heptanal: 5:1.

Table 5
Effect of temperature on selectivity to jasminaldehyde over 20% CHT/HMS.

Temperature (°C)	Conversion of benzaldehyde %	Selectivity to jasminaldehyde %
120	42.1	95.0
130	54.3	86.5
140	67.2	73.3
150	82.3	63.3

Conditions: catalyst loading: 0.1 g/cm^3, speed of agitation: 1200 rpm, benzaldehyde:heptanal: 5:1 (mol).

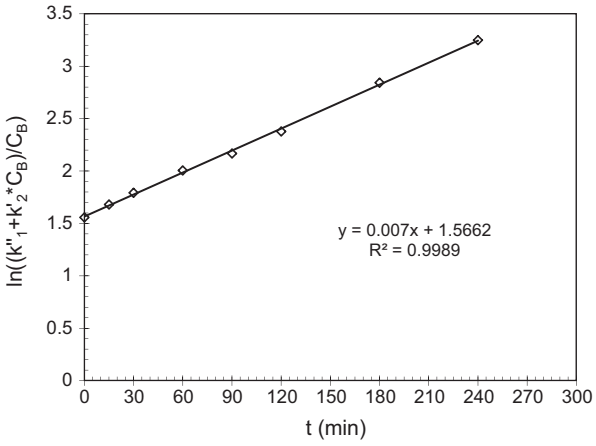

Fig. 11. Validity of the model: $\ln\{k_1'' + k_2' * C_B)/C_B\}$ versus time.

Thus, it is necessary to guess the values of rate constants and fit the data. k_1' and k_2 were calculated by using Polymath. It was found that the above model is valid (Fig. 11). A sample calculation, with an initial concentration of heptaldehyde $C_{B0} = 0.00154\,\text{kmol m}^{-3}$ at temperature 150 °C gives the following results. $k_1' = 0.007\,\text{min}^{-1}$, $k_2 = 0.2\,\text{m}^3\,\text{min}^{-1}\,\text{kmol}^{-1}$ and $k_1 = k_1'/C_{A0} = 0.007/0.0074 = 0.95\,\text{m}^3\,\text{min}^{-1}\,\text{kmol}^{-1}$. The above values show that the rate of aldol condensation is 4.75 times faster than the rate of self-condensation reaction on 20% CHT/HMS at 150 °C. Thus, the initial rate data of aldol condensation confirm that the rate constant so obtained matches well with that calculated by the Polymath method.

The rate constants for the aldol condensation were thus obtained at different temperatures by the polymath method. The Arrhenius plot was made for the aldol condensation (Fig. 12) to get the activation energy as 10.1 kcal/mol, which is lower than that for self-condensation. Invoking Eq. (30), it can be concluded that the use of lower temperature will reduce the by-product formation. Indeed, at 120 °C, the selectivity to jasminaldehyde was 95% although the reaction rate decreased considerably. Both these reactions are intrinsically kinetically controlled. Thus, the kinetic interpretation of the data is also correct.

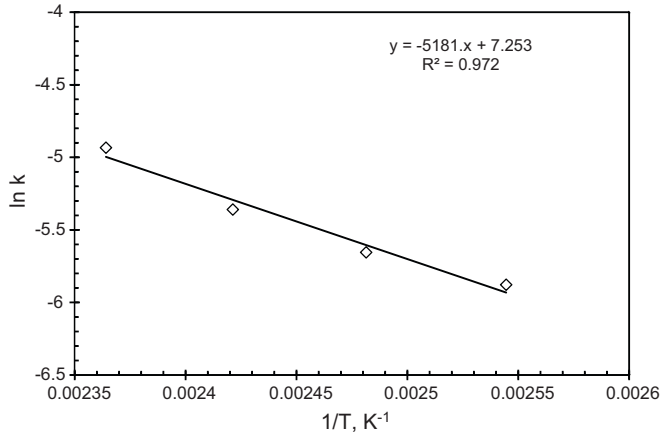

Fig. 12. Arrhenius plot for aldol condensation of benzaldehyde with heptanal.

4. Conclusion

A novel basic catalyst 20% (w/w) calcined hydrotalcite supported on hexagonal mesoporous silica (CHT/HMS) was synthesized and fully characterized by XRD, TG–DTA, pore size analysis, SEM–EDAX, and TEM. It possesses higher thermal stability, high adsorption capacity and large surface area. This catalyst shows excellent activity and selectivity in aldol-condensation of benzaldehyde with heptanal to jasminaldehyde. The overall reaction rate increases with increase in catalyst loading, reaction temperature and benzaldehyde to heptanal mole ratio. A kinetic model was developed and validated against experimental data. To get a very high selectivity, the optimum values of reaction parameters are: catalyst – 20% (w/w) CHT/HMS, catalyst loading – 0.1 g/cm^3 of liquid volume, heptanal to benzaldehyde mole ratio – 1:5, temperature −150 °C. The results are explained on the basis of the bifunctional character of CHT/HMS, where the role of the weak acid sites is the activation of benzaldehyde by protonation of the carbonyl group which favors the attack of the enolate heptanal intermediate generated on basic sites. The reaction was carried out without using any solvent to make process cleaner and greener. The catalyst has an excellent reusability.

Acknowledgements

GDY acknowledges support from the Darbari Seth Professor Endowment and R.T. Mody Endowment for personal chairs and Department of Science and Technology, Govt. of India, for the J.C. Bose National Fellowship. AP received Gujarat Ambuja SRF from Ambuja Research Institute.

References

[1] K. Tanabe, Solid Acids and Bases, Kodansha-Academic Press, New York, 1970.
[2] T.F. Degnan Jr., Top. Catal. 13 (2000) 349–356.
[3] K. Tanabe, M. Misono, Y. Ono, H. Hattori, New Solid Acids and Bases, Kodansha-Elsevier, Tokyo, 1989.
[4] H. Hattori, in: M. Guinet, J. Barrault, C. Bouchoul, D. Duprez, C. Montassier, G. Perot (Eds.), Heterogeneous Catalysis and Fine Chemicals III, Stud. Surf. Sci. Catal., vol. 78, Elsevier, Amsterdam, 1993, pp. 35–48.
[5] H. Hattori, Chem. Rev. 95 (1995) 537–550.
[6] F. King, G.J. Kelly, Catal. Today 2623 (2002) 1–7.
[7] S. Delsarte, A. Auroux, P. Grange, Phys. Chem. Chem. Phys. 2 (2000) 2821–2827.
[8] K. Weisssermel, H.J. Arpe, Industrial Organic Chemistry, 3rd ed., Wiley, New York, 1997, p. 273.
[9] K. Tanabe, W.F. Hoelderich, Appl. Catal. A: Gen. 181 (1999) 399–434.
[10] G.J. Kelly, F. King, M. Kett, Green Chem. 4 (2002) 392–399.
[11] F. Cavani, F. Trifiro, A. Vaccari, Catal. Today 11 (1991) 173–301.
[12] K. Koteswara Rao, M. Gravelle, J. Valente, F. Figueras, J. Catal. 173 (1998) 115–121.
[13] J.A. van Bokhoven, J.C.A.A. Roelofs, K.P. de Jong, D.C. Koningsberger, Chem. Eur. J. 7 (2001) 1258–1265.
[14] C.A. Hamilton, S.D. Jackson, G.J. Kelly, Appl. Catal. A: Gen. 263 (2004) 63–70.
[15] E. Angelescu, O.D. Pavel, R. Bîrjega, R. Zăvoianu, G. Costentin, M. Che, Appl. Catal. A: Gen. 308 (2006) 13–18.
[16] J.I. Di Cosimo, V.K. Díez, M. Xu, E. Iglesia, C.R. Apesteguía, J. Catal. 178 (1998) 499–510.
[17] M.V. Villa, M.J.S. Martin, M. S-Camazano, J. Environ. Sci. Health 1334 (1999) 509–514.
[18] T.M. Jyothi, T. Raja, M.B. Talawar, B.S. Rao, Appl. Catal. A: Gen. 211 (2001) 41–46.
[19] C.T. Kresge, M.E. Leonowicz, W.J. Roth, J.C. Vartuli, J.S. Beck, Nature 359 (1992) 710–712.
[20] S. Inagaki, Y. Fukushima, K. Kuroda, J. Chem. Soc. Chem. Commun. (1993) 680–682.
[21] P.T. Tanev, T.J. Pinnavaia, Science 267 (1995) 865–867.

[22] S.A. Bagshaw, E. Prouzet, T.J. Pinnavaia, Science 269 (1995) 1242–1244.
[23] D. Zhao, Q. Huo, J. Feng, B.F. Chmelka, G.D. Stucky, J. Am. Chem. Soc. 120 (1998) 6024–6036.
[24] K. Moller, T. Bein, Chem. Mater. 10 (1998) 2950–2963.
[25] J.H. Clark, D.J. Macquarrie, Chem. Commun. (1998) 1367–1370.
[26] A. Stein, B.J. Melde, R.C. Schroden, Adv. Mater. 12 (2000) 1403–1419.
[27] A. Sayari, S. Hamoudi, Chem. Mater. 13 (2001) 3151–3168.
[28] A. Sayari, Chem. Mater. 8 (1996) 1840–1852.
[29] C.A. Koh, R. Nooney, S. Tahir, Catal. Lett. 47 (1997) 199–203.
[30] I.V. Kozhevnikov, A. Sinnema, R.J.J. Jansem, K. Pamin, H. Van Bekkum, Catal. Lett. 30 (1995) 241–252.
[31] D.R. Patent 284, 458 (1927).
[32] L.S. Payne, European Patent 0392579 A2, 1990.
[33] P. Mastagli, G. Durr, Bull. Soc. Chim. Fr. (1955) 268–272.
[34] A. Sarkar, P.K. Dey, K. Datta, Indian J. Chem. B 25 (1986) 656–660.
[35] D. Abenhaim, C.P. Ngoc Son, A. Loupy, N. Ba Hiep, Synth. Commun. 24 (1994) 1199–1205.
[36] Y. Tanaka, N. Sawamura, M. Iwamoto, Tetrahedron Lett. 39 (1998) 9457–9460.
[37] S. Jaenicke, G.K. Chuah, X.H. Lin, X.C. Hu, Micropor. Mesopor. Mater. 35 (2000) 143–153.
[38] M.J. Climent, A. Corma, H. Garcia, R. Guil-Lopez, S. Iborra, V. Fornés, J. Catal. 197 (2001) 385–393.
[39] J.-I. Yu, S.Y. Shiau, A.-N. Ko, React. Kinet. Catal. Lett. 72 (2001) 365–372.
[40] P.T. Tanev, T.J. Pinnavia, Science 267 (1995) 865–867.
[41] W.T. Reichile, J. Catal. 94 (1985) 547–557.
[42] W. Wie, H. Peng, L. Chen, J. Mol. Catal. A: Chem. 246 (2006) 24–32.
[43] R.M. Queiroz, L.H.O. Pires, R.C.P. de Souza, J.R. Zamian, A.G. de Souza, G.N. da Rocha Filho, C.E.F. da Costa, J. Therm. Anal. Calorim. 97 (2009) 163–166.
[44] F. Cavani, F. Trifiro, A. Vaccari, Catal. Today 11 (1990) 173–301.
[45] E.I. Kamitosos, A.P. Patsis, G. Kordas, Phys. Rev. B-48 (1993) 12499–12505.
[46] F. Cavani, F. Trifiro, A. Vaccari, Catal. Today 11 (1991) 201–206.
[47] K.S.W. Sing, D.H. Everett, R.A.W. Haul, L. Mouscou, R.A. Pierotti, J. Rouquerol, T. Siemieniewska, Pure Appl. Chem. 57 (1985) 603–619.
[48] S. Velu, M. Shah, T.M. Jothi, S. Sivasanker, Micropor. Mesopor. Mater. 33 (1999) 61–75.
[49] M.J. Climent, A. Corma, S. Iborra, A. Velty, J. Catal. 221 (2004) 474–482.
[50] X. Lei, F. Zhang, L. Yang, X. Guo, Y. Tian, S. Fu, F. Li, D.G. Evans, X. Duan, AIChEJ 53 (2007) 932–940.
[51] H.S. Folger, Elements of Chemical Reaction Engineering, 3rd ed., Prentice Hall, New Jersey, 1999, p. 636.